

MC-ISTA-Net: Adaptive Measurement and Initialization and Channel Attention Optimization inspired Neural Network for Compressive Sensing

Nanyu Li¹, Cuiyin Liu^{1,*}, Wei Dai¹

¹ Computer Key Laboratory of Yunnan Province

Faculty of Information Engineering and Automation

Kunming University of Science and Technology

e-mails:908204990@qq.com, liucuiyin@kmust.edu.cn, daiwei@astrolab.cn

ABSTRACT

The optimization inspired network can bridge convex optimization and neural networks in Compressive Sensing (CS) reconstruction of natural image, like ISTA-Net⁺, which mapping optimization algorithm: iterative shrinkage-thresholding algorithm (ISTA) into network. However, measurement matrix and input initialization are still hand-crafted, and multi-channel feature map contain information at different frequencies, which is treated equally across channels, hindering the ability of CS reconstruction in optimization-inspired networks. In order to solve the above problems, we proposed MC-ISTA-Net: First, we remove the nuisance parameter on ISTA-Net⁺, and completed the simultaneous training of measurement matrix, input initialization and optimization inspired network through fully connected layers, so training measurement matrix can extract the information of scene more efficiently to improve CS reconstruction, adaptive initialization can avoid complicated prior calculations to improve training speed. Furthermore, we use the one-dimensional convolution channel attention mechanism to get more powerful features. Experiments show that MC-ISTA-Net out perform better than state-of-the-art CS methods in CS reconstruction without sacrificing speed, and is also attractive in performance when we compared to image Super Resolution.

Index Terms— Optimization Inspired Network, Simultaneous Training, Measurement Matrix, Input Initialization, Channel Attention

1. INTRODUCTION

Unlike Shannon's theory, Compressed Sensing (CS) theory[1-2] demonstrates that a signal allowing for data sampling rate much lower than Shannon sampling rate can be reconstructed with high probability when it is sparse in itself or in some transform domain. This new technology is very hardware-friendly, reducing the cost of sampling and even increasing the speed of imaging, thus having a wide range of mature applications in many fields, such as fast Magnetic Resonance Imaging (MRI)[3], fast and low-dose X-ray

imaging [4], radio astronomy imaging [5], single pixel camera [6], 3D-video [7]. In this paper, we focus on CS reconstruction of natural images, but our framework can be generalized to other image and video. CS reconstruction is generally seen as a convex optimization problem [2], and there are many fast and accurate traditional methods, such as Alternating Direction Method of Multipliers (ADMM) [8], fast iterative shrinkage-thresholding algorithm (FISTA)[9], iterative shrinkage-thresholding algorithm (ISTA) [9], approximate message passing (AMP) [10]. However, the traditional convex optimization algorithm has the following shortcomings. It not only needs to manually set the optimization parameters, the measurement matrix and transform by a priori, but also needs hundreds of iterations to get the optimal solution.

With the rise of deep neural networks, people began to consider the relationship between it and compressed sensing. We hope that data-driven neural networks can avoid manual setting of optimization parameters through end-to-end training. The powerful abilities of feature extraction and generalization of deep neural networks can handle the optimal transform, even measurement matrix, input initialization in CS. There are two mainstream ways now, one that uses neural networks completely. Such as Ali Mousavi[11] directly uses a stacked auto-encoder to handle CS reconstruction. Kuldeep [12] proposed ReconNet, using convolutional network to handle CS reconstruction. Further, Hantao Yao [13] proposed DR2-Net, which uses the residual network to deal with CS. The other is similar to the differentiable programming [14], called optimization inspired network, training the optimization parameters, and using the neural network instead of the fixed transform to learn the optimal transform with sparsity. Such as Christopher A. Metzler proposes an LAMP [15], inspired AMP optimization algorithm that based on data-driven to learn optimization parameters. Zongben Xu [3] proposed ADMM-Net, mapping ADMM algorithm into a deep network, using the circular convolution to learn linear optimal transform. Recently, Jian Zhang proposed ISTA Net[16], mapping ISTA optimization algorithm into a deep network, based on the universal approximation principle, they use two convolution layers and a rectified linear unit

(ReLU) activation function to achieve a nonlinear optimal transform. Furthermore, they proposed ISTA-Net⁺ [16], add a linear operators which are composed of convolutional layers, introducing residual connections to reduce training difficulty. Because of optimization-inspired design, ADMM Net, ISTA Net and ISTA-Net⁺ are generally better than ordinary neural networks in CS reconstruction, and convergence speed. However, features of different channels also contain information about the different frequencies of the reconstructed image in optimizing inspired networks. The above model lack channel-wise attention to learn features discriminately. In addition, all optimization inspired networks still manually selects the measurement matrix and initialization.

In this paper, we propose an adaptive measurement and initialization and channel attention neural network which mapping ISTA algorithm into a deep neural network for CS, dubbed MC-ISTA-Net: we use fully connected layers to adaptively learn the measurement matrix, and input initialization of network. The channel attention mechanism based on convolutional network evaluates the reconstruction feature of different frequencies to improve the representational ability of network.

Contribution: Our contributions are four-fold. (1) We develop a channel attention mechanism based on small convolution to improve CS reconstruction. (2) We have reduced the parameters of the original ISTA-Net⁺, but model does not degrade. (3) We implemented the measurement matrix, input initialization and CS reconstruction to train simultaneously. (4) Our proposed MC-ISTA-Net not only achieves high performance in compressed sensing, but is also attractive when we compared with state of the art methods from image Super Resolution.

2. RELATED WORK

We systematically introduce the traditional ISTA algorithm for CS, ISTA-inspired neural network, and analyze the connection and development between them.

Traditional ISTA for CS reconstruction: Given the under sampled measurement $y \in R^{M \times M}$, the traditional CS reconstruction methods (AMP, ADMM, ISTA, FISTA) obtains the original image $x \in R^{M \times M}$ by solving the following Eq. (1):

$$\min_{x \in R^{N \times N}} \|y - Gx\| + \lambda \|D(x)\|_1 \quad (1)$$

$G \in R^{M \times N}$ is the measurement matrix ($M \ll N$), $\frac{M}{N}$ is CS ratios (under sampling ratios). $D(x)$ denotes the transform coefficients of x with respect to some fixed transform D (such as FFT[18], DWT[19], DCT[20]), and the sparsity of each vector of $D(x)$ is encouraged by the ℓ_1 norm with λ being the regularization parameter. G , D , λ need to be pre-defined.

The traditional ISTA [9] can only get $D(x)$, but Yunsong Liu, [17] proposes projected ISTA which get x directly, introducing a canonical dual frame to construct an orthogonal projection operator: $D^T(D(x)) = x$. Based on proximal

mapping, projected ISTA solves Eq. (1) by iterating between the following update steps (r is the intermediate reconstruction):

$$r^{(k)} = x^{(k-1)} - \beta G^T(Gx^{(k-1)} - y) \quad (2)$$

$$x^{(k)} = D^T(\text{soft}(D(r^{(k)}), \theta)) \quad (3)$$

Here, k is the iterative index of the projected ISTA, β is the step size, θ is the threshold of the shrinkage threshold function, and D is the fixed transform. Compared to the ADMM, AMP, etc. algorithm, this method still out-performs the state-of-the-art at that time. However, all parameters (in addition to k) need to be pre-defined based on image prior, and very challenging to tune a priori. Fixed transform usually cannot exhibits stable sparsity for all images of the dataset, especially natural images, and results in poor reconstruction performance.

ISTA inspired Deep Network: Bridging the projected ISTA and deep convolutional networks can solve the above problem, Jian Zhang proposed ISTA-Net[16], unrolling the ISTA method (k phase), **the transform module** $D^{(k)}$ consists of two convolution layers and ReLU activation function in Phase (iteration) k . Compared to the circular convolution of ADMM-Net, it can learn nonlinear transform from dataset. And all optimization parameters are trainable, and not shared in each k phase. Because of the orthogonality of the projected ISTA, the loss function of the symmetry constraint is additionally introduced:

$$L_{\text{symmetry}} = \|D^{(k)T}(D^{(k)}(x^{(k)})) - x^{(k)}\|_2^2 \quad (4)$$

Furthermore, inspired by a residual structure of image[21], Jian Zhang proposed ISTA-Net⁺: a linear operator $H^{(k)}$ which includes $3 \times 3 \times 32$ convolution kernels to increase the number of channels. The linear operator $L^{(k)}$ which includes $3 \times 3 \times 1$ convolution kernels to reduce the number of channels, and uses residual connections to reduce the training difficulty of the network. This structure achieves the same effect of Nesterov acceleration [16] of FISTA (in our experiments). Every phase in ISTA-Net⁺ is:

$$r^{(k)} = x^{(k-1)} - \beta^{(k)} G^T(Gx^{(k-1)} - y) \quad (5)$$

$$x^{(k)} = L^{(k)} D^{(k)T}(\text{soft}(D^{(k)}(H^{(k)}(r^{(k)})), \theta^{(k)})) + r^{(k)} \quad (6)$$

However, ISTA-Net⁺, ISTA-Net has the following disadvantages: Input initialization $x^{(0)}$, need to calculate the entire training set, which has a high computational risk:

$$Q = XY^T(Y Y^T)^{-1} \quad (7)$$

$$x^{(0)} = Qy \quad (8)$$

X is all images of the training set, Y is for all under sampling measurements, and Q is the initialization matrix. In our experiments, selecting other hand-crafted input initialization often leads to network degradation. Moreover, Measurement matrixes of almost all CS methods (ISTA-Net⁺, ISTA-Net, ADMM-Net, L-AMP, ReconNet and SDA,etc) are hand-crafted, which may ignore the interdependence of measurement matrices and CS reconstruction, Furthermore,

these networks treat the channel-wise features equally, which contain information about the different frequencies of reconstructed pictures, hindering better discriminative ability for different types of features, which is the bottleneck for further performance improvement of CS.

3. PROPOSED MC-ISTA-NET

In order to solve the above problems to improve the performance of CS reconstruction, as shown in Fig.1, we proposed MC-ISTA-Net. In addition to the layers of adaptive measurements and input initialization, MC-ISTA-Net contains deep structure of 1 to K phases by unrolling the ISTA method, the structure of each phase is same: $x^{(k)}$, $r^{(k)}$ are the reconstructed image and intermediate reconstruction in each phase(index is k). $x^{(K)}$ is the final reconstructed image. Compared to ISTA-Net⁺, we use the same transform module, $H^{(k)}$ and $L^{(k)}$ has changed, canceled the fixed measurement matrix and initialization, added two fully connected layers, and channel attention module.

Because the purposes of $H^{(k)}$ and $L^{(k)}$ only focus on channel transformation, we developed the structure of the ISTA-Net⁺ by using 1×1 convolution kernels instead of 3×3 convolution kernels in $H^{(k)}$ and $L^{(k)}$ but without degrading the model. (As shown in 4.3). Furthermore, our proposed network allows the measurement matrix, input initialization and CS reconstruction network to be trained simultaneously and automatically select more favorable features through the channel attention mechanism.

3.1. Adaptive Measurement and Initialization

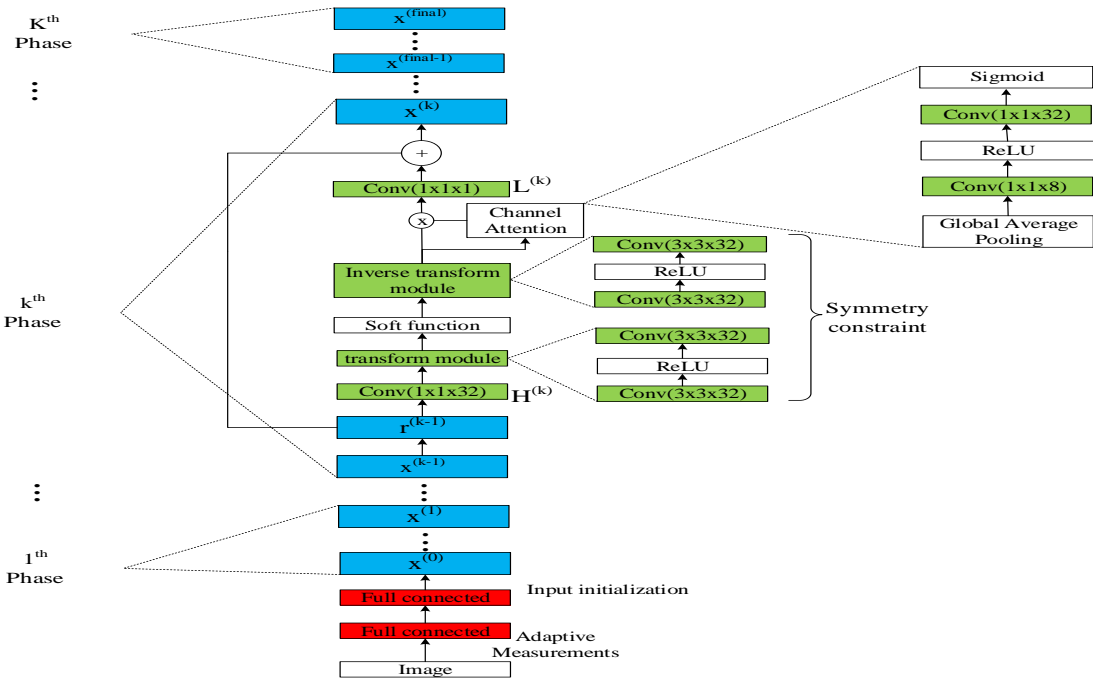


Fig.1 illustration of our proposed MC-ISTA-Net framework

Almost all CS methods (including traditional optimization method, network based method, and optimization inspired network) usually use a fixed measurement matrix, such as orthogonal Gaussian matrix [22], orthogonal Fourier matrix[23]. However, just as training transform can improve reconstruction, adaptive measurement matrix [24] can fits dataset better and extract the information of scene more efficiently and get better reconstruction results. Optimization-based network usually use complex input initialization to improve CS (introduced in 2), but adaptive initialization can solve this shortcoming. Furthermore, in CS theory, measurement matrix, initialization and transform need to work together [2][25] (such as restricted isometry property (RIP) condition [26] demonstrate that the structures of measurement matrix and the optimal transform should be no coherent), so simultaneous training [27] that enables adaptive measurement, initialization, and training transform to work together to achieve to better reconstruction

Now, we'll give you more details on how to implement adaptive measurements and input initialization with some fully connected layers. As shown in Figure 1, we use a fully connected layer with zero bias, the input is the image, the output is the under sampling measurement, the dimension of the output set according to the CS rate, and the training weight is the measurement matrix. Similarly, add another fully connected layer with zero bias. The input is an under sampling measurement and the output is the input of initialization of the CS reconstruction network:

$$y = F(x, W_G) \quad (9)$$

$$x^{(0)} = F(y, W_Q) \quad (10)$$

F is a fully connected layer, W_G, W_Q are the training weights which correspond to the adaptive measurement matrix G and initialization matrix Q respectively. Our network bridges the CS reconstruction, measurement matrix and input initialization not only does not require complex initialization calculations, and hand-crafted measurement matrix but also improves CS performance

3.2. Channel Attention

We know that no one now uses attention mechanisms to improve CS reconstruction. However, from $H^{(k)}$ to $L^{(k)}$ (in Fig.1), different types of convolution kernels can generate different channels feature maps, and these feature map also can correspond to different frequency representations of the image on the convex optimization, and simple convolutional networks cannot focus on interdependencies between different channels, so paying attention to evaluating this dependence can improve the CS reconstruction. Inspired by [28], for each Phase, before the linear operator $L^{(k)}$, we introduce the channel attention mechanism, use global average pooling [29] to get global spatial information, and then use different channel numbers of 1×1 convolution filters, and the ReLU function, to rescale of the channel-wise feature, and use the sigmoid function to get the channel-wise attentional representation, which is expressed as follows:

$$C^{(k)} = D^{(k)T}(\text{soft}(D^{(k)}(H^{(k)}(r^{(k)})), \theta^{(k)}) \quad (11)$$

$$a^{(k)} = \text{sigmoid}(f_w(\text{relu}(f_u^{(k)}(C^{(k)}))) \quad (12)$$

$$x^{(k)} = L^{(k)}(C^{(k)} \times a^{(k)}) + r^{(k)} \quad (13)$$

$C^{(k)}$ is the feature which needs attention, its numbers of channels is w . After global average pooling, we use two stacked convolution layers to rescale features, the channel numbers of first convolutional layer is $\frac{w}{u}$ (u is the compression factor, is 4 in Fig.1 and Fig.2) and activation function σ is ReLU; the channel numbers and activation function of second convolutional layer are w and sigmoid respectively. Unlike

the SE-Net[30] which widely used in computer vision tasks, we replaced the fully connected network with a one-dimensional convolution network, as shown in Figure 2:

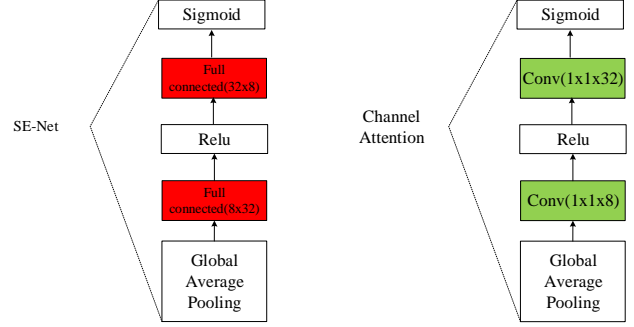


Fig.2 The structure of SE-Net and Channel Attention

As shown in Fig.2, because Channel Attention uses one-dimensional convolution structure[31], the size of parameters is much lower than SE-Net(SE-Net uses two full connection layers with $32 \times 8 + 8 \times 32 = 512$ parameters, Channel Attention uses two one-dimensional convolution layers with $32+8=40$ parameters)

3.3. MC-ISTA-Net

In summary, we give the loss function and training parameters of MC-ISTA-Net, like ISTA-Net⁺[16], our total loss function is as follows (including symmetry constraint loss):

$$L_{\text{all}} = \|x^{(\text{final})} - x^{(k)}\|_2^2 + \tau \|D^{(k)T}(D^{(k)}(x^{(k)})) - x^{(k)}\|_2^2 \quad (14)$$

The regularization parameter τ need to pre-defined, and Training parameters of network include:

$$\{W_G, W_Q, \beta^{(k)}, \theta^{(k)}, H^{(k)}, D^{(k)}, D^{(k)T}, L^{(k)}, a^{(k)}\}$$

(all optimization parameters are not shared in each k phase.) Our Adaptive measurement, initialization, and attention mechanisms can also be easily extended to other methods such as ADMM-Net, LAMP, etc. to improve their performance.

Tab.1 Average PSNR(dB) performance comparisons on Set 11

Algorithm	CS ratio							Time CPU/GPU	FPS CPU/GPU
	50%	40%	30%	25%	10%	4%	1%		
D-AMP[10]	35.92	33.56	30.39	28.46	22.64	18.40	5.21	51.21s/--	0.36/--
ReconNet[12]	31.50	30.58	28.74	25.60	24.28	20.63	17.27	--/0.016s	/62.5
A-ReconNet[21]	33.21	32.72	31.23	30.80	27.53	23.22	20.33	--/0.016s	--/62.51
DR2-Net[13]	32.4	31.2	30.52	28.66	24.71	20.08	17.44	--/0.87s	--/32.3
ADMM-Net[3]	36.89	34.96	32.62	30.97	25.76	21.22	17.29	1.5s/---	2.7/--
ISTA-Net[16]	37.43	35.36	32.91	31.53	25.80	21.23	17.30	0.923s/0.039s	1.08/25.6
ISTA-Net ⁺ [16]	38.07	36.06	33.82	32.57	26.64	21.31	17.34	1.375s/0.047s	0.73/21.3
MC-ISTA-Net	39.53	37.34	35.09	33.81	28.51	24.31	19.48	1.360s/0.043s/	0.72/21.4

1. EXPERIMENTAL RESULTS

1.1. Settings

The experiments are performed on a workstation with Intel Core i7-6820 CPU and a GTX-Titan XP.

Training settings: For the fair comparison, follow common practices in previous CS work, we use the same 91 images of the data set from [12] as training: random extract luminance component of 8912 randomly cropped image block (each of size 33×33) of the image set. According to different CS ratios: $\{1\%, 4\%, 10\%, 12.5\%, 25\%, 30\%, 33.3\%, 40\%, 50\%\}$, training separately MC-ISTA-Net. We use Tensorflow to implement and use Adam optimization with a learning rate 0.0001, a batch size of 64, the model's Phase=9, $\tau=0.001$.

Testing settings: Following[10-13,16], we use two standard benchmark datasets for testing in CS: Set 11[12], BSD68[32], for better performance measurement, compare with methods from other reconstruction tasks, such as image Super Resolution(SR)[33] in the benchmark datasets: BSDS100[32]

Evaluation metric : PSNR is used for evaluating CS reconstructs results and SR results. 1,000 images from Image Net CLS-LOC validation dataset were used for evaluation.

1.2. Comparison in CS Reconstruction

We compared our model MC-ISTA-Net with nine recent and state-of-the art image CS methods: D-AMP[10], ReconNet[12], DR2-Net[13], Adaptive ReconNet[21] (A-ReconNet), ADMM- Net [8], ISTA-Net[16], ISTA-Net+[16]. The first one is optimization-based methods, the second and third are networks-based methods, and the last three are interpretable optimization-inspired network-based methods. The average PSNR reconstruction performance on Set11 dataset with respect to seven CS ratios are summarized in Tab.1.

Tab.2 Average PSNR(dB) performance comparisons on BSD68

Algorithm	CS Ratios				
	50%	40%	30%	10%	4%
SDA[11]	28.35	27.41	26.38	23.12	21.32
ReconNet[12]	29.86	29.08	27.53	24.15	21.66
ISTA-Net[16]	33.60	31.85	29.93	25.02	22.12
ISTA-Net+[16]	34.01	32.21	30.34	25.33	22.17
MC-ISTA-Net	35.74	33.81	31.92	27.27	24.65

From Tab.1, we observed that ADMM-Net, ISTA-Net, and ISTA-Net+ benefited from the optimization-inspired design, achieving almost better performance than other comparing methods, while the traditional optimization-based algorithm works better at high CS sampling rates. While network-based algorithms perform better at low CS sampling rates, especially Adaptive ReconNet. However, our proposed MC-ISTA-Net almost out perform all the existing methods across all the CS ratios and the last two columns show the

average time to reconstruct per-image and the corresponding frames-per-second (FPS, the greater value of FPS, the faster the speed), so our model does not sacrifice speed. Further, we compare with SDA, ReconNet, ISTA-Net, and ISTA-Net⁺ on larger BSD68 dataset with respect to five CS ratios are summarized in Tab.2 As shown in Table 2, validating the generalizability of our MC-ISTA-Net in larger dataset. Our model still surpasses other models under all CS ratios.

1.3. Ablation Studies

In this section, we study the effect of small convolution in $H^{(k)}$ and $L^{(k)}$ Channel Attention and adaptive measurement (as introduced in 3.1-3) in our MC-ISTA-Net and compared with other similar structures, such as SE Net [30], Soft Channel Attention (using a soft threshold function [34] instead of sigmoid function), as shown in Tab.3, where the experimental setup: using Adam optimization with a learning rate 0.0001, a batch size of 64, the model's Phase = 9, CS ratio = 25%, dataset is Set11. The comparison algorithm is as follows: S-ISTA-Net (using two The 1×1 small convolution filter to replace the 3×3 convolution filter of the original ISTA-Net⁺ in $L^{(k)}$, $H^{(k)}$), FISTA-Net(add Nesterov acceleration [16] of FISTA for the original ISTA-Net⁺), A-ISTA-Net (replaced a two-layer fully connected network with orthogonal Gaussian measurement matrix and initialization calculation in ISTA-Net⁺), SE-ISTA-Net (introducing an SE-Net[30] for A-ISTA-Net), Soft-ISTA-Net (similar to MC-ISTA-Net, The soft threshold function is used instead of the original sigmoid function in Channel Attention)

Tab.3 Ablation Studies

Algorithm	CS Ratios	
	25%	32.57
ISTA-Net ⁺ [16]		
S-ISTA-Net		32.57
FISTA-Net		32.56
A-ISTA-Net		33.47
Soft-ISTA-Net		33.55
SE-ISTA-Net		33.79
MC-ISTA-Net		33.81

As shown in Tab.3, compared to the original ISTA-Net+. We found that S-ISTA-Net does not causing degradation of the model; Both Adaptive measurement and Channel Attention improve network performance. In particular, our Channel Attention performs better than SE-Net, with fewer model parameters, and the poor performance of soft Channel Attention may be due to the fact that the output of the soft threshold function is more likely to cause loss of the feature of the channel information.

1.4. Comparison with Super Resolution

Although image super-resolution and CS reconstruction belong to different reconstruction tasks, they based on the same idea, both can be regarded as ill-conditioned problems[2], recovering high-dimensional details from low-dimensional information. The comparison between CS

method(our model, ADMM-Net[3],ReconNet[12]) and SR method (RCAN⁺[28], SPMSR[36], IRCNN[35]) And SPMSR is also an optimized based method, ADMM and MC-ISTA-Net are optimization inspired network, the other is the Network based method. Our experiment is expressed in the standard benchmark datasets: BSDS100.

Tab.4 Average PSNR in BSDS 100

Algorithm	Size reduction	×2/50 %	×3/33 %	×4/25 %	×8/12.5 %
SPMSR[44]	BD	-	25.84	-	-
IRCNN[35]	BD	30.98	28.62	27.29	24.53
ReconNet[12]	CS	30.27	26.46	23.72	20.88
ADMM[3]	CS	31.21	28.27	26.67	25.01
RCAN ⁺ [28]	BI	32.46	29.32	27.85	25.05
MC-ISTA-Net	CS	35.28	32.09	30.53	27.67

As shown in Tab.4, for fair comparison, based on the same size reduction, the ratio of upscaling corresponds to the CS ratios. The results show that the reconstruction effect of our model is better than all other models, which may be because: compared to BI/BD degradation model, CS under sampling exists a higher probability of reconstructing high-dimensional images from low-dimensional inputs mathematically; and structure of optimization inspired network has more powerful representation than structure of ordinary neural network and optimized method. However, image super-resolution usually is more flexible than CS reconstruction in real life.

1.5. Object Recognition Performance

The object recognition performance is experimented and evaluated which further demonstrate the effectiveness of our MC-ISTA-Net. We use Res Net-50 [37] as the evaluation model and use the first 1,000 images from Image Net CLS-LOC validation dataset: The original cropped 224×224 images are used for baseline; downscaled to 56×56 for SR methods; and the CS sampling rate is 25% and the input is 56×56 for CS methods. Our model MC-ISTA-Net is compared with the state of art SR method: RCAN⁺[28], IRCNN[35], CS method: ADMM-Net[3].

Tab.5 ResNet object recognition performance

Evaluation	IRCNN[35]	ADMM-Net[3]	RCAN ⁺ [28]	MC-ISTA-Net	Baseline
Top1-error	0.476	0.402	0.381	0.350	0.260
Top5-error	0.251	0.192	0.159	0.144	0.072

As shown in Tab.5, our method achieves the lowest top-1 and top-5 errors. These comparisons further demonstrate the highly powerful and meaningful representational ability of our MC-ISTA-Net.

2. CONCLUSIONS

An adaptive measurement and initialization and channel attention ISTA inspired neural network (MC-ISTA-Net) was proposed to improve reconstruction performance of compressive sensing of natural images. The nuisance parameter on ISTA-Net⁺ was removed, input initialization and optimization was realize by fully connected layers and with simultaneous training of measurement matrix. So training measurement matrix can extract the information of scene more efficiently to improve CS reconstruction, adaptive initialization can avoid complicated prior calculations to improve training speed. Furthermore,

One-dimensional convolution channel attention mechanism is used to get more features. The result of experiments in the paper show that MC-ISTA-Net has attain progress in CS reconstruction, Super Resolution and object performance, etc. The extended research work will be carried out in the future.

3. ACKNOWLEDGE

This work is supported by National Natural Science Foundation of China (NSFC) "Research on registration methods of solar multi-band ground-space images" (11773012), the National Key Research and Development Program of China (2018YFA0404603, 2016YFE0100300), the Joint Research Fund in Astronomy (No.U1531132, U163129, U1831204) under cooperative agreement between the National Natural Science Foundation of China (NSFC) and the Chinese Academy of Sciences (CAS), the National Natural Science Foundation of China (No.11403009 and 11463003). Yunnan Natural Science Foundation (2017FB001). The major scientific research project of Guangdong regular institutions of higher learning (2017KZDXM062).

4. REFERENCES

- [1] Donoho D L Compressed sensing[J]. IEEE Transactions on Information Theory, 2006, 52(4):1289-1306.
- [2] Candes E J, Tao T. Near-Optimal Signal Recovery From Random Projections: Universal Encoding Strategies?[J]. IEEE Transactions on Information Theory, 2006, 52(12):5406-5425.
- [3] Yan Y, Huibin L, Zongben X , et al. Deep ADMM-Net for compressive sensing MRI[J]. Advances in Neural Information Processing Systems.
- [4] Yoseop Han, Jaejoon Yoo, Jong Chul Ye: Deep Residual Learning for Compressed Sensing CT Reconstruction via Persistent Homology Analysis [J] IEEE Conference on Computer Vision and Pattern Recognition
- [5] Wenger S, Magnor M, Y. Pihlström, et al. SparseRI: A Compressed Sensing Framework for Aperture Synthesis Imaging in Radio Astronomy[J]. Publications of the Astronomical Society of the Pacific, 2010, 122(897):1367-1374
- [6] Duarte M F , Davenport M A , Takhar D , et al. Single-Pixel Imaging via Compressive Sampling[J]. IEEE Signal Processing Magazine, 2008, 25(2):83-91.

[7] Edgar M P , Gibson G M , Spalding G C , et al. Real-time 3D video utilizing a compressed sensing time-of-flight single-pixel camera[C] Optical Trapping & Optical Micromanipulation XIII. Optical Trapping and Optical Micromanipulation XIII, 2016.

[8] Boyd S , Parikh N , Chu E , et al. Distributed Optimization and Statistical Learning via the Alternating Direction Method of Multipliers[J]. Foundations & Trends in Machine Learning, 2010, 3(1):1-122.

[9] Beck A , Teboulle M . A Fast Iterative Shrinkage-Thresholding Algorithm for Linear Inverse Problems[J]. SIAM Journal on Imaging Sciences, 2009, 2(1):183-202.

[10] Schniter P , Rangan S , Fletcher A . Denoising based Vector Approximate Message Passing[J]. 2016.

[11] Mousavi A , Patel A B , Baraniuk R G . A Deep Learning Approach to Structured Signal Recovery[J]. 2015.

[12] Kulkarni K , Lohit S , Turaga P , et al. ReconNet: Non-Iterative Reconstruction of Images from Compressively Sensed Random Measurements[J]. 2016.

[13] Yao H , Dai F , Zhang D , et al. DR2-Net: Deep Residual Reconstruction Network for Image Compressive Sensing[J]. 2017.

[14] Gregor K , Lecun Y . Learning fast approximations of sparse coding[C] International Conference on International Conference on Machine Learning. Omnipress, 2010.

[15] Borgerding M , Schniter P , Rangan S . AMP-Inspired Deep Networks for Sparse Linear Inverse Problems[J]. IEEE Transactions on Signal Processing, 2017:1-1.

[16] Zhang J , Ghanem B. ISTA-Net: Iterative Shrinkage-Thresholding Algorithm Inspired Deep Network for Image Compressive Sensing[J]. 2017.

[17] Liu Y , Zhan Z , Cai J , et al. Projected Iterative Soft-thresholding Algorithm for Tight Frames in Compressed Sensing Magnetic Resonance Imaging[J]. IEEE Transactions on Medical Imaging, 2016:1-1.

[18] Hua S , Ding M , Yuchi M. Sparse-view ultrasound diffraction tomography using compressed sensing with nonuniform FFT[J]. Computational and Mathematical Methods in Medicine, 2014,(2014-4-24), 2014, 2014(2):329350.

[19] Zhang J , Xia L , Huang M , et al. Image reconstruction in Compressed Sensing based on single-level DWT[C]// IEEE Workshop on Electronics, Computer & Applications. IEEE, 2014.

[20] Stankovic L , Brajovic M. Analysis of the Reconstruction of Sparse Signals in the DCT Domain Applied to Audio Signals[J]. IEEE/ACM Transactions on Audio Speech & Language Processing, 2018, PP(99):1-1.

[21] Sullivan G J , Ohm J R , Han W J , et al. Overview of the High Efficiency Video Coding (HEVC) Standard[J]. IEEE Transactions on Circuits & Systems for Video Technology, 2013, 22(12):1649-1668.

[22] Wang B , Ma S X. Improvement of Gaussian Random Measurement Matrices in Compressed Sensing[J]. Advanced Materials Research, 2011, 301-303:245-250.

[23] Fannjiang A . Compressive Inverse Scattering with TV-min and Greedy Pursuit[J]. 2012.

[24] Xie X , Wang Y , Shi G , et al. Adaptive Measurement Network for CS Image Reconstruction[J]. 2017.

[25] Liang J , Sch önlieb, Carola-Bibiane. Faster FISTA[J]. 2018.

[26] Nelson J , Price E , Wootters M. New constructions of RIP matrices with fast multiplication and fewer rows[J]. Computer Science, 2012.

[27] Hickson R C. Interference of strength development by simultaneously training for strength and endurance[J]. European Journal of Applied Physiology & Occupational Physiology, 1980, 45(2-3):255.

[28] Zhang Y , Li K , Li K , et al. Image Super-Resolution Using Very Deep Residual Channel Attention Networks[J]. 2018.

[29] Lin M , Chen Q , Yan S . Network In Network[J]. Computer Science, 2013.

[30] Hu J , Shen L , Albanie S , et al. Squeeze-and-Excitation Networks[J]. 2017.

[31] Xu Y , Cheng J , Lei W , et al. Ensemble One-Dimensional Convolution Neural Networks for Skeleton-Based Action Recognition[J]. IEEE Signal Processing Letters, 2018, 25(7):1044-1048.

[32] Martin D , Fowlkes C , Tal D , et al. A database of human segmented natural images and its application to evaluating segmentation algorithms and measuring ecological statistics[C]// Proceedings Eighth IEEE International Conference on Computer Vision. ICCV 2001. IEEE, 2002.

[33] Park S C , Min K P , Kang M G. Super-resolution image reconstruction: a technical overview[J]. IEEE Signal Processing Magazine, 2003, 20(3):21-36.

[34] Zhang L , Wang H , Xu Y. A shrinkage-thresholding method for the inverse problem of Electrical Resistance Tomography[C]// Instrumentation & Measurement Technology Conference, 2012.

[35] Zhang K , Zuo W , Gu S , et al. Learning Deep CNN Denoiser Prior for Image Restoration[J]. 2017.

[36] Peleg, T, Elad, M.: A statistical prediction model based on sparse representations for single image super-resolution. TIP (2014)

[37] He, K., Zhang, X., Ren, S., Sun, J.: Deep residual learning for image recognition. In: CVPR. (2016)